applied sciences

Article

# Improving Quality Control Methods to Test Strengthening Technologies: A Multilevel Model of Acoustic Pulse Flow

**Egor Grigorev [1,*] and Viktor Nosov [1,2]**

[1] Department of Metrology, Instrumentation and Quality Management, Saint Petersburg Mining University, 199106 Saint-Petersburg, Russia; nosovvv@list.ru
[2] Peter the Great St. Petersburg Polytechnic University, 195251 Saint-Petersburg, Russia
* Correspondence: grigorev_ev@pers.spmi.ru

**Abstract:** This article describes an approach that makes it possible to substantiate quality control criteria and methods to improve strengthening technologies. The approach was used to test the quality of products made using these technologies and analyze different strengthening methods applied to structural materials. In the experiment, samples of welded joints subjected to various types of strengthening were used that underwent acoustic emission (AE) testing. The results of quick evaluations produced by the proposed multilevel model of acoustic pulse flow were compared with the results of long-term cyclic tests to make a conclusion about the effectiveness of the approach being discussed. To improve strengthening quality control, a method is proposed that can be applied to complex and large-sized structures in the construction industry.

**Keywords:** strengthening technologies; acoustic emission; information and kinetic approach; multilevel model; concentration and kinetic criteria; welded joints

check for updates

**Citation:** Grigorev, E.; Nosov, V. Improving Quality Control Methods to Test Strengthening Technologies: A Multilevel Model of Acoustic Pulse Flow. *Appl. Sci.* **2022**, *12*, 4549. https://doi.org/10.3390/app12094549

Academic Editor: Giuseppe Lacidogna

Received: 22 March 2022
Accepted: 27 April 2022
Published: 30 April 2022



## 1. Introduction

As reliability requirements in engineering are becoming more stringent, it is necessary to enhance and upgrade structural materials [1,2] and technologies with a view to improving their performance properties. Different industries use a huge variety of strengthening technologies depending on the type of the material. Their ultimate goal is to extend the service life of the item under test, and they all have certain advantages and disadvantages [3–5]. Whether the application of one or another strengthening technology on a particular product will be successful depends on many factors and can be assessed by testing strength reliability parameters, which is a time-consuming task.

Structural materials can be strengthened by means of various methods (mechanical, thermal, chemical, etc.) at different steps of the production process [6–8], leading to an irreversible improvement in strength parameters. They include different force, deformation, or structural parameters that do not necessarily have direct relationships with the most objective indicators of the long-term strength of a real object [9]. Applying strengthening technologies can change the size of the structural element or cause a decrease in residual stresses, which does not always lead to an increase in the object's service life. Therefore, it is necessary to be able to assess the impact of each individual strengthening technology in a quick and non-destructive way.

Nondestructive testing (NDT) methods used to assess the quality of strengthening technologies can be classified by the type of controlled signal and its connection with the processes that determine the strength of the material. Methods relying on signals that are recorded as a result of waves being transmitted and reflected [10–12] cannot provide an unambiguous picture of the object's strength parameters or the process of damage growth; they miss nanoscale information as waves bend around strength anomalies. Such methods record signals that mainly provide information about the reflectivity of large structural elements rather than about the strength of the material. It is therefore necessary to move from testing the spatial parameters of structural elements, such as their shape, size, and orientation in space, to temporal parameters reflecting the process of damage accumulation and affecting its service life.

NDT methods that are based on recording wave parameters associated with the process of damage to the material include electromagnetic (eddy current) testing (ET) and acoustic emission (AE) testing [13–15]. As the application of strengthening technologies results in heterogeneous strength parameters of the material due to, for example, the redistribution of internal stresses, this affects how informative NDT methods are in reflecting the material's service life. Due to this, the key issue associated with the application of AE methods in strength testing is the complexity of interpreting the signals and connecting the results with strength parameters. When dealing with items that have been subjected to the complex influence of strengthening technologies, strength measurement results in many uncertainties. However, it is important to have measurement methods that produce adequate and reliable results. This article proposes a solution to this problem based on identifying the relationship between the results of AE tests and the parameters of the item under study with further estimation of the residual service life.

The article aims to provide a rationale for a quick NDT method for studying the results of applying strengthening technologies. The method is based on the information and kinetic approach to interpreting the results of recording acoustic signals and was tested on welded joints.

## 2. Materials and Methods

The problem discussed above can be solved by means of mathematical models that remove uncertainty when describing the real physical process. They should rely on universal constants and accurately measured parameters that are representative.

### 2.1. Information and Kinetic Approach

A distinctive feature of this approach is that, rather than record the acoustic emission signal first, the physical processes are first modeled to assess the current state of the test object by means of concentration and kinetic indicators of the AE process and universal physical constants found by processing the results of AE tests and using reference s–n curves.

The method uses a multilevel model [16] based on fracture micromechanics, the kinetic concept of strength, and the statistical regularities of elastic wave radiation. The strength and AE parameters of structural materials are the result of superposition and depend on the results of fracturing and plastic deformation processes simultaneously occurring in the material.

The diagram of the multilevel model is created with its mathematical description being expressed by Equation (1) [16]. The multilevel model of acoustic pulse flow parameters combines statistical and physical approaches to testing. It allows for obtaining information that reduces the uncertainty of strength properties at the macro-, micro-, and nano-levels of strength tests to make a reasonable choice of AE indicators. The approach is described in more detail in [16,17], but it is the first time it has been applied to quality control in the area of strengthening technologies.

$$\xi(t) = k_{AE}C(t) = V\int\int\int_{\Delta t,f,u}\Phi(\Delta t,f,u)dudfd\Delta tC(t), \quad (1)$$

where $\xi$ is the primary informative AE parameter (number of pulses, relative amplitude, energy, etc.); $k_{AE}$ is the acoustic emission coefficient; $C(t)$ is the concentration of fractured structural elements; $V$ is the volume of the material being tested; $\Phi(\Delta t, f, u)$ is the probability density of the distribution of AE signals by intervals $\Delta t$ between them, frequency $f$, and amplitude $u$. Given the stochastic nature of elastic wave radiation, the triple integral included in the expression has the meaning of detection probability, that is, the probability that the parameters of elastic waves coming from the AE source fall into the range of frequencies, AE signal amplitudes, and time intervals recorded by the measuring device.

The approach is based on the idea that the test object is a combination of structural elements whose individual states determine the state of the object as a whole. The strength indicator is the time until the structural elements become fractured, which is described by the Zhurkov formula [18–20], and the key factor determining the moment of fracturing is the rate of damage accumulation until reaching a critical value. As the strength parameters of the material are not homogeneous, the equation for describing the growth in the concentration of fractured elements has the following form:

$$C(t) = C_0 \int_{\omega_0}^{\omega_0+\Delta\omega} \Psi(\omega)\left\{1 - exp\left[-\int_0^t \frac{dt'}{\theta_{avg}}(U_0, \omega(t))\right]\right\}d\omega, \tag{2}$$

where $C_0$ is the initial concentration of structural elements in the material before failure; $\omega_0$ is the lower limit of the range of $\omega$; $\Delta\omega$ is a representative dispersion range of $\omega$ values by structural elements; $\Psi(\omega)$ is the distribution density function of the values of $\omega$ by structural elements; $\theta_{avg}$ is the average time before one structural element fails, which is found by the Zhurkov formula; $U_0$ is the energy that activates the process of fracturing; $\omega = \gamma\sigma/KT$ is the strength parameter of the structural element, where: $\gamma$ is the activation volume [21,22] (nanostructure parameter); $\sigma$ is tensile stresses in the structural element; $K$ is the Boltzmann constant; and $T$ is the absolute temperature.

The ratio between the parameters of the function $\Psi(\omega)$ reflects how heterogeneous the strength parameters of the material are. Several options for modeling the function $\Psi(\omega)$ are used [16], including using two weights (0.99 ÷ 0.999 and 0.01 ÷ 0.001).

$$\Psi(\omega, \omega_0, \omega_1, \omega_2) = \begin{cases} \frac{0{,}99}{\omega_1}, \omega \in [\omega_0, \omega_0 + \omega_1]; \\ \frac{0{,}01}{\omega_2}, \omega \in [\omega_0 + \omega_1, \omega_0 + \omega_1 + \omega_2] \end{cases} \tag{3}$$

The heterogeneity is associated with variations in the mechanical properties of structural elements and is of a stochastic nature, which makes it impossible to use the model for accurate failure prediction. To solve the problem, prediction can be reduced to extrapolating the time dependence between the concentration of microcracks and time onto its critical value. To do it, it is necessary to identify the stage in the process of fracturing that signals future failure by means of filtering signals corresponding to the fracture of the most durable elements of the material that have similar strength parameters from signals that reflect elements ranging in their strength parameters. The criterion for such filtration is the kinetic uniformity of the fracture in the structural elements. Identified through the temporal filtering of AE signals, the stage of uniform fracturing makes it possible to register signals associated with the failure of strong structural elements that are responsible for how long the test object will serve its purpose. It is essential that the parameters of the model of the fracturing process for representative structural elements determined at this stage correlate with the parameters of the s–n curves, which confirms the relationship between the s–n curves and the damage that is expressed in the form of the damage accumulation hypotheses and is the basis for linking the measurement results with the reliability parameters.

According to [16,17], sections of the time curve for the number of AE pulses $N_{\sum}(t)$ recorded under the stress at the stage of uniform fracturing with a constant rate of stress growth $\dot{\sigma}$ are described by the expression:

$$N_{\Sigma}(t) = k_{AE} C_0 KT \cdot exp\left[\frac{\gamma\dot{\sigma}t - U_0}{KT}\right] / \left(\tau_0 \gamma \dot{\sigma}\right) \tag{4}$$

By linking the parameters of acoustic emission with the parameters of microscopic failure under the correct stress ($k_{AE}$ = const, with stress occurring at a constant rate of a stress growth $\dot{\sigma} \neq 0$ and stability of the amplitude distribution of AE signals being observed), the model makes it possible to formulate strength parameters in such domains as energy, structure, and time at macro-, micro-, and nanolevels and to formulate criteria for assessing the quality of strengthening technologies (Table 1).

**Table 1.** Concentration and kinetic parameters of acoustic emission for assessing the quality of strengthening technologies [16].

| AE Indicator | Micromodel | Nanomodel | Macromodel |
|---|---|---|---|
| $X_{AE}$ ($s^{-1}$) | $d\ln\xi/dt$ | $\gamma\dot{\sigma}/KT$ | - |
| $Y_{AE}$ ($Pa^{-1}$) | $d\ln\xi/d\sigma$ | $\gamma/KT$ | $d\ln Nc/d\sigma$ * |
| $W_{AE}$ | $d\ln\xi/dKs$ ** | $\omega = \gamma\sigma/KT$ | $\ln N_B$-$\ln N_{cw}$ * |

* $N_c$, $N_B$, and $N_{cw}$ are s–n curve parameters of the material; ** $K_s$ is the stress factor (ratio of test stress to working stress).

Each of the proposed criteria, or indicators, has a clear physical significance and is calculated using the results of recording AE signals from the elastic deformation zone at the stage of uniform fracturing. The proposed method improves testing accuracy by tracking changes in both the structure and the stress state of a real product. It links the proposed criteria for assessing the quality of strengthening technologies with the key strength parameters of materials and is compatible with standard (based on s–n curve parameters) methods for assessing strength and service life. The differences are in the algorithms used and in the application of the criteria.

$$N_c = \frac{N_B}{expW_{AE}} \tag{5}$$

where $N_B$ is the characteristic parameter of the material, temperature, and frequency of its stress, which is found from the s–n curve of samples made of this material (reference value).

### 2.2. *Strengthening Technologies and Stress Device*

As the test object, welded joints were chosen, since they are the most vulnerable elements of structures operating under long-term cyclic loads. S-n curves of welded joints show differences in the impact that the welded joint zone has on the resistance to long-term cyclic loads and short-term failure loads. The service life of objects operating under low tension is limited by their welded joints. Therefore, it is necessary to monitor only the fracturing of those structural elements of the welded joint that affect service life.

The proposed approach was tested on steel plate samples with welded joints. The plates were made of the ST3PS steel (similar to steel A 414 Grade A) with the following dimensions: 150 × 25 × 4 mm. By means of semi-automatic welding, welded joints were made on both sides in the middle of the sample. The samples were divided into four groups and strengthened using three technologies: heat treatment [23–27], ultrasonic treatment [28–30], and structural hardening by means of beveling [31,32].

The first group of samples included plates that were not treated.

In the second group, heat treatment (tempering) was applied to relieve residual stresses in welded joints. The operation was carried out in a SNOL 7.2/1100 muffle furnace by heating the samples at a rate of 10 °C per minute until the temperature reached 600 °C. This temperature was maintained for two hours, after which the samples were left to cool in the furnace. During high tempering, hardness parameters decrease and become homogeneous, while plasticity and impact strength increase, with residual stresses decreasing by 70% to 80%.

In the third group, the welded joints on the samples were subjected to ultrasonic impact treatment (UIT) at a frequency of 20.1 kHz and a power of 200 watts.

In the fourth group, beveling was performed on both sides of the plates. Beveling promotes stronger welds and reduces the welding time.

The samples were stressed using a Zwick/Roell Z100 universal testing machine, which creates uniform tension. Figure 1 shows the samples and the equipment that were used in the experiment. The results were processed using the approach described above.

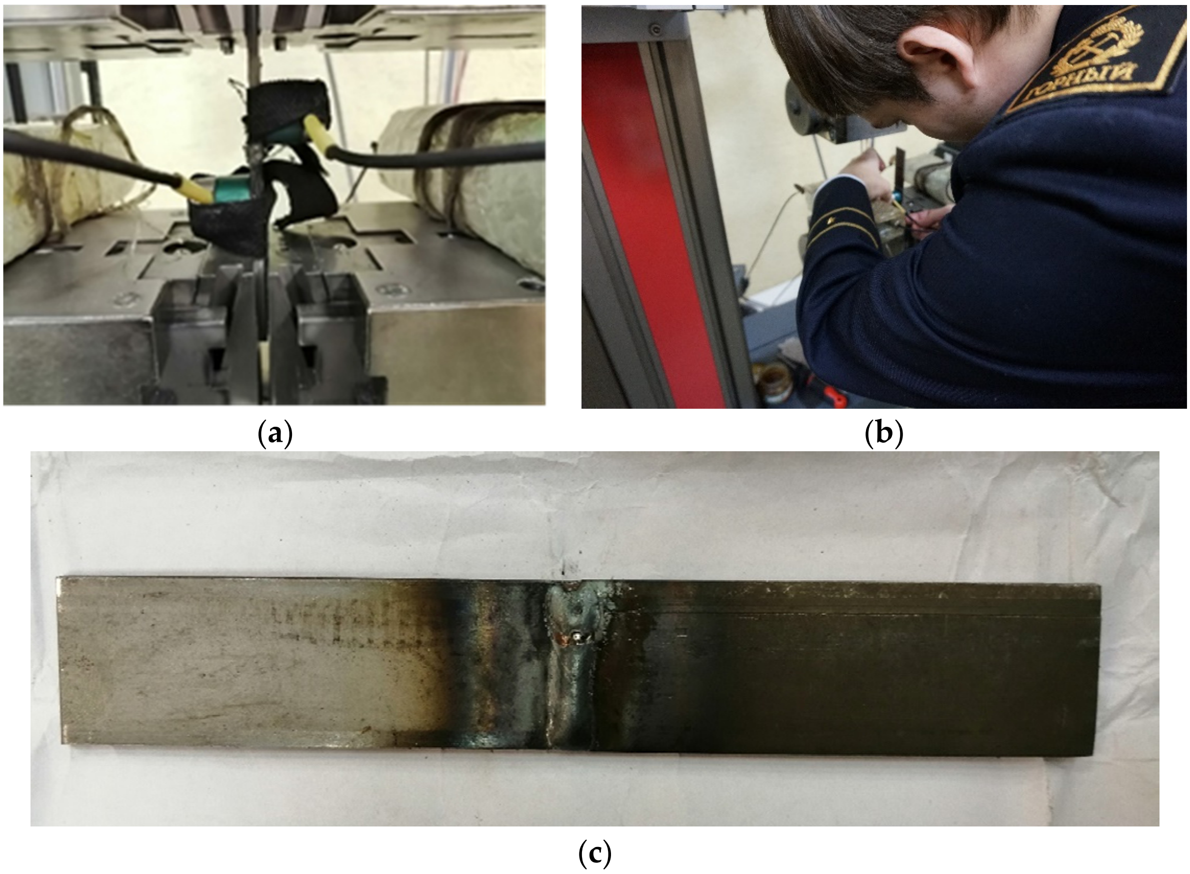


**Figure 1.** The process of conducting the experiment. (**a**,**b**) Equipment and acoustic emission transducers located on the sample and the process of acoustic emission recording. (**c**) A typical sample of the ST3PS steel.

For registration of AE signals, a dual-channels acoustic emission system SDAE with 2 TAE P113c type was used. The extended frequency range of the registered signals was 20–1000 kHz. The lower level of the system discrimination threshold was determined by the need to eliminate electromagnetic interference and was 47 dB on each channel; the blocking time was 48,000 µs, which made it possible to register microcracks larger than 100 µm. A range of digital parameters characterizing the signals coming from the preamplifier was transmitted via the CAN2.OB interface in the computer. The scheme of running the experiment is shown in Figure 2.

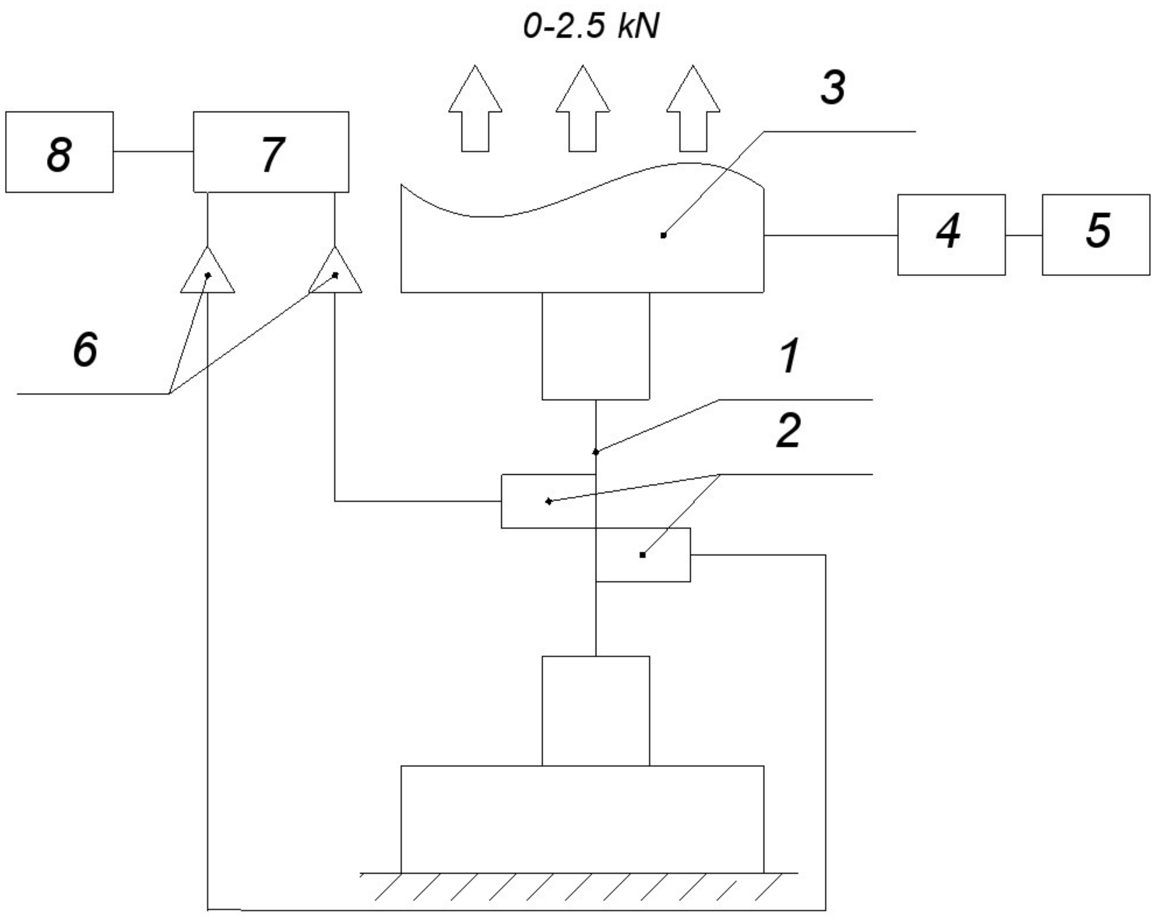


**Figure 2.** Functional scheme of loaded device 1—sample; 2—transducers of acoustic emission (TAE); 3—universal testing machine; 4—control unit; 5—computer for load management; 6—preamplifier of AE signals; 7—AE signals processing unit; 8—computer for registration of AE signals.

## 3. Results and Discussion

The samples were subjected to tension until failure. In the process, acoustic emission was recorded. In all the samples, the failure occurred in the metal free from welds, which is why the mechanical properties of the plates rather than those of the welds were measured. Since strengthening technologies were mainly applied to the welds, and it was from the welds that AE signals were recorded, the authors decided that the results of processing AE information should be compared not with the results of static failure tests, but with the results of fatigue tests in samples being fractured along the welds.

The experiment produced an array of acoustic emission data, which was processed according to the method described above for finding concentration and kinetic indicators (Table 1) at the stage of uniform fracturing in the elastic deformation zone. This zone was chosen as a zone of correct stress, since it corresponds to uniform stress in the range of operating stresses of a given material in a real object in many industrial areas. The results of recording the key AE parameters at the stage of elastic wave radiation are shown in Figure 3.

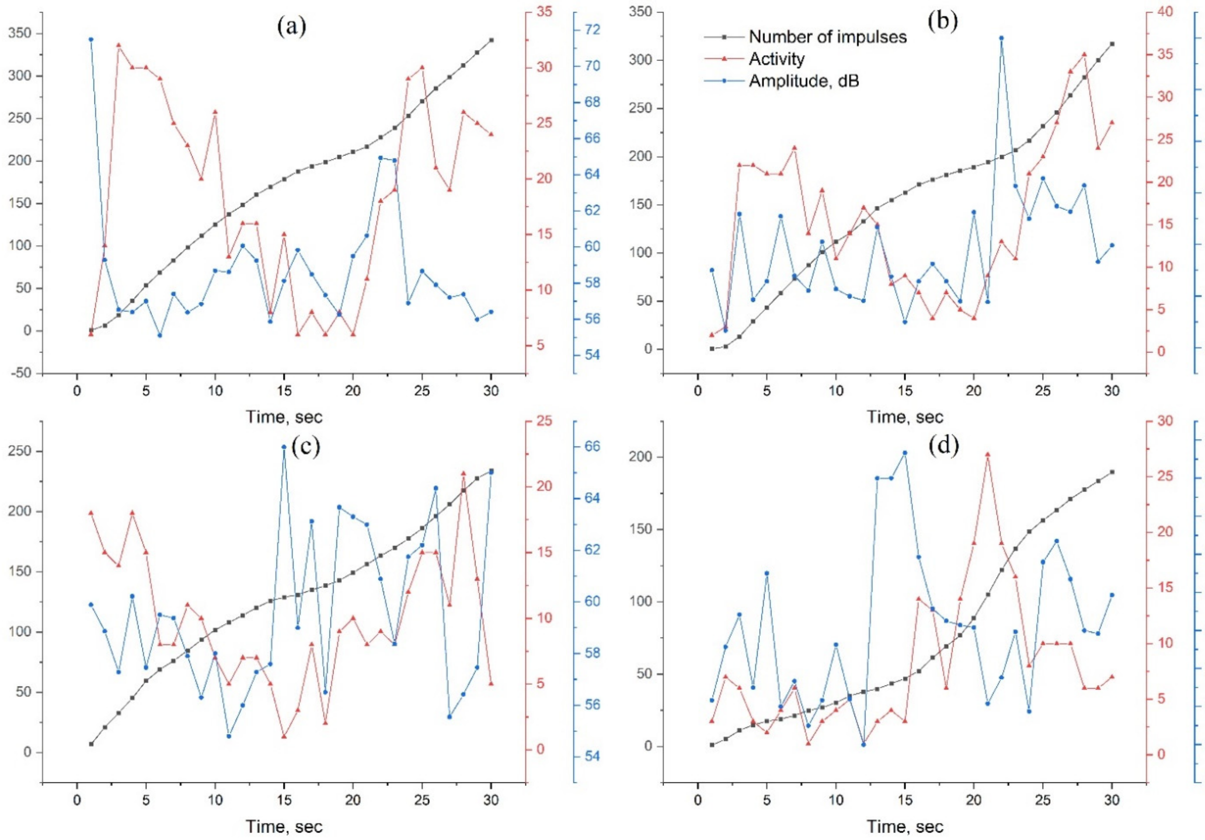


**Figure 3.** Key AE indicators as functions of time at the stage of elastic deformations, where (**a**) is an untreated sample, (**b**) is a sample after heat treatment, (**c**) is a sample after beveling, (**d**) is a sample after ultrasonic treatment.

The limits of the uniform fracturing period were found by comparing the results of failure simulation (Equation (2)) with a constantly increasing stress and the experimental results of recording AE parameters (Equation (1)), under the condition that $\xi$ and $C(t)$ are proportional ($k_{AE}$ = const). Figure 4 shows an example of finding the limits of the uniform fracturing period. For each of the samples at this stage, such parameters were found as the values of the concentration and kinetic strength indicators using the formulas from Table 1, MARSE (Measured Area under the Rectified Signal Envelope), which corresponds to energy (according to the energy and statistical approach to AE testing) [33,34], the average value of the amplitude, the number of pulses, and AE activity. To assess how informative the proposed method is, a correlation analysis was performed, where the correlation was found between the resulting values of concentration and kinetic indicators and traditional AE indicators (number of pulses, MARSE, etc.) and the number of cycles to failure of welded joint samples during fatigue tests, which were obtained using similar samples from the same material and the same strengthening technologies [35]. The results are shown in Table 2. The service life of the samples was calculated using Equation (5), with the value of the working stress being taken in the range of 50 to 100 MPa, as this is the average working stress in various industrial areas.

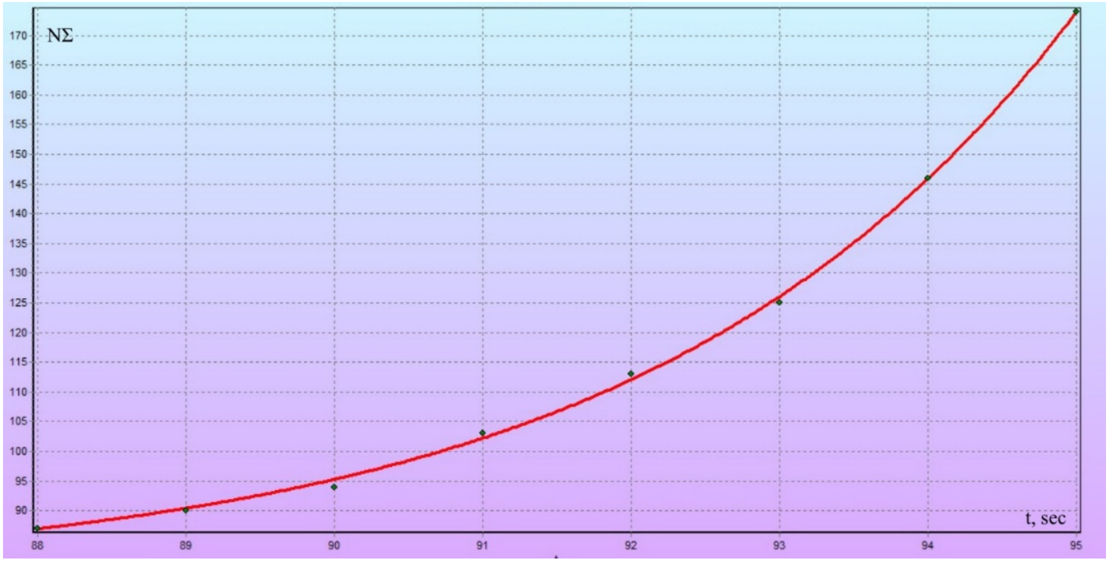


**Figure 4.** Comparing the results of failure simulation modeling (Equation (4)) (red line) and the number of AE pulses (dots) to find the limits of the uniform fracturing period using one of the samples as an example. Based on this, we find the values of the quality criterion $X_{AE}$ as the ratio of the logarithm of the number of pulses at the beginning and end of the uniform fracturing period to the duration of this period ($\ln N_2$-$\mathrm{Ln} N_1/t_2$-$t_1$ = 4.673–4.043/95–88 = 0.09 $s^{-1}$).

**Table 2.** Correlation coefficients for the average values of the concentration and kinetic indicators and the average values of the key acoustic emission indicators.

| Strengthening Technology/Average Parameter Value | Untreated Samples | Ultrasonic Treatment | Beveling | Heat Treatment | Correlation Coefficient for the Number of Cycles to Failure |
|---|---|---|---|---|---|
| $X_{AE}$, $s^{-1}$ | 0.066 | 0.054 | 0.036 | 0.024 | −0.992 |
| $Y_{AE}$, $MPa^{-1}$ | 0.0049 | 0.0042 | 0.0028 | 0.0012 | −0.999 |
| $W_{AE}$ | 0.548 | 0.349 | 0.260 | 0.152 | −0.934 |
| MARSE, $mV^2 \cdot ms$ | 121,011 | 139,038 | 234,456 | 243,607 | 0.993 |
| Number of pulses (N) | 75 | 120 | 188 | 243 | 0.982 |
| Amplitude, mV | 58.2 | 59.5 | 57.7 | 58.6 | 0.055 |
| Activity, 1/N | 7.8 | 9.9 | 15.7 | 18.6 | 0.995 |
| Increase in service life, % | 0 | 22 | 25 | 48 | - |
| Number of cycles to failure from [35] | 2951 | 4246 | - | 10,399 | - |

Table 2 shows that the heat-treated samples have the highest number of pulses, activity, and MARSE, which means that there is a lot of noise and it is impossible to assessing strengthening quality using these parameters. In addition, these parameters have a positive correlation with service life, which goes against their physical significance. However, the proposed concentration and kinetic indicators make it possible to assess strengthening quality by factoring in the influence of noise, which proves their resistance to destabilizing factors. The negative value of the correlation coefficient describing the relationship between the concentration and kinetic criteria and the service life corresponds to all previously obtained results, demonstrating the stability of the relationship, which cannot be said about traditional criteria, including MARSE [33].

The results of the experiment show that as a function of time, the number of AE pulses in the hardened samples has an atypical form, with a period of attenuation in the middle of the stage of elastic deformations. As can be seen in Figure 3, activity sharply stops, which is explained by the fact that large elements from the "tail" zone of the $\Psi(\omega)$ distribution

(Equation (3)) stopped emitting, and there is a complete absence of signals (Figure 5). From the point of view of the model used, this is interpreted by smoothing or even separating the "tail" from the "bell" of the $\Psi(\omega)$ distribution, with a further shift of the "bell" to the region of small values of $\omega$. The general distribution, which had both "bell" and "tail" shapes, smoothed out, i.e., strengthening caused medium-strength elements to move into the "bell" zone, and the values of $\Psi(\omega)$ in the "tail" region decreased. A decrease in $\Psi(\omega)$ to zero corresponds to the separation of the "tail" from the "bell". The presence of a plateau in the time function of the number of AE pulses was substantiated by the gap between the "bell" and the "tail" of the $\Psi(\omega)$ distribution. Such a gap can be the result of strengthening operations removing internal stresses from heterogeneous elements that have values of $\omega$ in the "tail" part of the $\Psi(\omega)$ distribution. Since these elements do not determine the service life of the material, such removal does not lead to strengthening, which explains the distrust in methods for assessing the quality of strengthening technologies based on internal stress testing, which is carried out by reflection or scattering methods on large elements of the "tail" that are more conducive to both reflection and scattering.

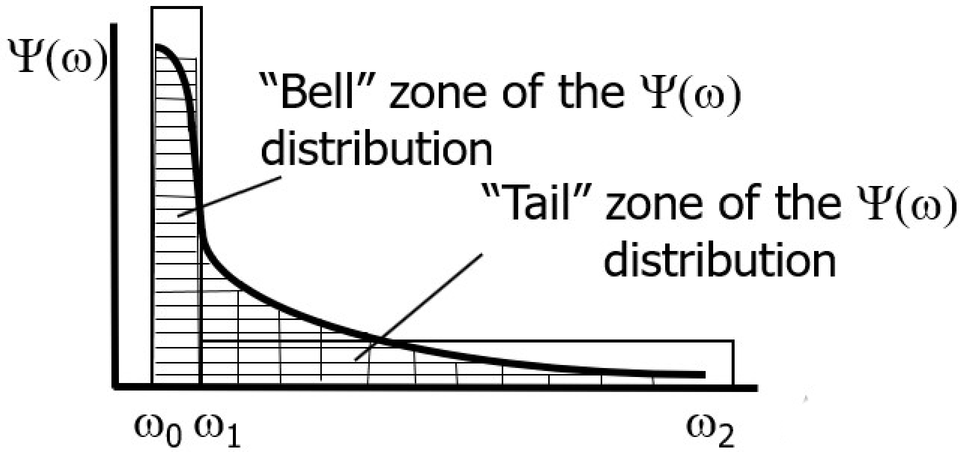


**Figure 5.** Typical distribution $\Psi(\omega)$ (two-dimensional modeling of $\omega$).

By comparing the experimental curve and the simulation curve (Equation (2)), we can conclude that the "tail" is separated from the "bell" of the distribution. The first AE signals demonstrate kinetically heterogeneous fracturing with high $\omega$ values of the $\Psi(\omega)$ distribution function. Then, there is a period of attenuation, after which the "bell" begins to manifest itself, i.e., the elements begin to "sound" at the stage of uniform fracturing, where the values of the times to fracture measured by AE signals have high values, with a minimum value of the strength parameter of the $\Psi(\omega)$ distribution function.

As the concentration and kinetic parameters do not depend on the volume of the test object, it suggests that they can be used in testing real-life objects that can be subjected to hydrotests or pneumatic tests.

## 4. Conclusions

As a result of the research performed on welded joints, an information and kinetic approach was proposed for assessing strengthening quality. The following conclusions were made:

1. The method proposed in this article is based on a multilevel model of AE parameters and allows for performing quick evaluations of strengthening quality. The approach can be used as a foundation for making the optimal choice of strengthening operations to be applied to real-life items.
2. Strengthening occurs where the values of concentration and kinetic indicators ($X_{AE}$, $Y_{AE}$, $W_{AE}$) decrease. The lower the values of the indicators, the higher the strengthening, and the better the results produced by the technology.

3. High AE activity in samples hardened by heat treatment signals that the traditionally used statistical indicators for assessing strengthening quality are not very informative.
4. The results showed that with the specified heat treatment parameters, the service life of the welded joint increases by 48%, while with UIT it increases by 25%.

**Author Contributions:** Conceptualization, E.G. and V.N.; methodology, V.N.; formal analysis, E.G.; resources, E.G. and V.N.; data curation, E.G.; writing—original draft preparation, E.G.; writing—review and editing, V.N.; visualization, E.G.; supervision, V.N. All authors have read and agreed to the published version of the manuscript.

**Funding:** This research received no external funding.

**Institutional Review Board Statement:** Not applicable.

**Informed Consent Statement:** Not applicable.

**Data Availability Statement:** Not applicable.

**Conflicts of Interest:** The authors declare no conflict of interest.

## References

1. Smirnova, O.; Kazanskaya, L.; Koplík, J.; Tan, H.; Gu, X. Concrete based on clinker-free cement: Selecting the functional unit for environmental assessment. *Sustainability* **2021**, *13*, 135. [CrossRef]
2. Smirnova, O.M.; de Navascués, I.M.P.; Mikhailevskii, V.R.; Kolosov, O.I.; Skolota, N.S. Sound-absorbing composites with rubber crumb from used tires. *Appl. Sci.* **2021**, *11*, 7347. [CrossRef]
3. Xiong, Z.; Timokhina, I.; Pereloma, E. Clustering, nano-scale precipitation and strengthening of steels. *Prog. Mater. Sci.* **2021**, *118*, 100764. [CrossRef]
4. Zampieri, P.; Simoncelo, N.; Tetougueni, C.D.; Pellegrino, C. A review of methods for strengthening of masonry arches with composite materials. *Eng. Struct.* **2018**, *171*, 154–169. [CrossRef]
5. Wong, L.N.Y.; Zhang, Y.; Wu, Z. Rock strengthening or weakening upon heating in the mild temperature range? *Eng. Geol.* **2020**, *272*, 105619. [CrossRef]
6. Liu, G.; Huang, C.; Zhao, B.; Wang, W.; Sun, S. Effect of Machined Surface Integrity on Fatigue Performance of Metal Workpiece: A Review. *Chin. J. Mech. Eng. Engl. Ed.* **2021**, *34*, 118. [CrossRef]
7. Olugbade, T.O.; Ojo, O.T.; Omiyale, B.O.; Olutomilola, E.O.; Olorunfemi, B.J. A review on the corrosion fatigue strength of surface-modified stainless steels. *J. Braz. Soc. Mech. Sci. Eng.* **2021**, *43*, 421. [CrossRef]
8. Sheinerman, A.G. Plastic deformation and fracture processes in metal/graphene composites: A review. *Crit. Rev. Solid State Mater. Sci.* **2021**, 1–28. [CrossRef]
9. *GOST 18295-72*; Surface Working. Terms and Definitions. State standard of the union of the SSR: Moscow, Russia, 1973. (In Russian)
10. Dive, V.; Lakade, S. Recent research progress on residual stress measurement using non-destructive testing. *Mat. Tod. Proc.* **2021**, *47*, 3282–3287. [CrossRef]
11. Trofimov, A.V.; Rumyantsev, A.E.; Gospodarikov, A.P.; Kirkin, A.P. Non-destructive ultrasonic method of testing the strength of backfill concrete at deep talnakh mines. *Tsvetn. Met.* **2020**, *12*, 28–32. [CrossRef]
12. Potapov, A.I. Estimation of the relation of strength and ultrasound speed in glass-reinforce plastic. *J. Min. Inst.* **2018**, *230*, 176–184. [CrossRef]
13. Rasskazov, I.Y.; Tsirel', S.V.; Rozanov, A.O.; Tereshkin, A.A.; Gladyr', A.V. Application of acoustic measurement data to characterize initiation and development of disintegration focus in a rock mass. *J. Min. Sci.* **2017**, *53*, 224–231. [CrossRef]
14. Kozak, K.; Bućko, M.M.; Chlubny, L.; Lis, J.; Antou, G.; Chotard, T. Influence of composition and grain size on the damage evolution in MAX phases investigated by acoustic emission. *Mater. Sci. Eng. A* **2019**, *743*, 114–122. [CrossRef]
15. Kozak, K.; Dosi, A.; Bućko, M.M.; Chlubny, L.; Lis, J.; Antou, G.; Chotard, T. Investigation of the mechanical behavior of MAX phases by acoustic emission technique. *Mater. Sci. Eng. A* **2017**, *707*, 73–80. [CrossRef]
16. Nosov, V.V. On the principles of optimizing the technologies of acoustic-emission strength control of industrial objects. *Russ. J. Nondestr. Test.* **2016**, *52*, 386–399. [CrossRef]
17. Nosov, V.V. Appraising the Service Life of Dangerous Engineering Equipment by Acoustic Emission Diagnosis. *J. Mach. Manuf. Reliab.* **2020**, *49*, 1072–1083. [CrossRef]
18. Fedotov, S.N. Quasi-brittle fracture as failure of hierarchical structure. *Fizich. Mezom.* **2015**, *6*, 24–31. (In Russian) [CrossRef]
19. Moghanlou, M.R.; Khonsari, M.M. On the kinetic formulation of fracture fatigue entropy of metals. *Fatigue Fract. Eng. Mater. Struct.* **2022**, *45*, 565–577. [CrossRef]
20. Sirota, D.Y. A new kinetic model for the long-term strength and geo-composite materials. *Mining. Inf. Anal. Bull.* **2014**, *4*, 222–225. (In Russian)

21. Plotnikov, V.A.; Makarov, S.V. Activation volume and acoustic emission at high-temperature deformation of aluminum. *Tamb. Uni. Rep. Ser. Nat. Tech. Sci.* **2010**, *15*, 1068–1071. (In Russian)
22. Gorbatykh, V.P.; Ivanov, S.O. To definition of the activation volume parameter in the limits of the kinetic theory of durability. *Vest MEI. Bull. Mos. Pow. Engin. Inst.* **2010**, *3*, 16–19. (In Russian)
23. Matlock, D.K.; Kang, S.; De Moor, E.; Speer, J.G. Applications of rapid thermal processing to advanced high strength sheet steel developments. *Mater. Charact.* **2020**, *166*, 110397. [CrossRef]
24. Milyuts, V.G.; Tsukanov, V.V.; Pryakhin, E.I.; Nikitina, L.B. Development of manufacturing technology for high-strength hull steel reducing production cycle and providing high-quality sheets. *J. Min. Inst.* **2019**, *239*, 536–543. [CrossRef]
25. Bezyazychnyi, V.F.; Szcerek, M. Thermal processes research development in machine-building technology. *J. Min. Inst.* **2018**, *232*, 395–400. [CrossRef]
26. Lipin, V.A.; Trufanov, D.A. Effect of chalk thermal treatment mode on its strength. *J. Min. Inst.* **2019**, *236*, 210–215. [CrossRef]
27. Bazhin, V.Y.; Issa, B. Influence of heat treatment on the microstructure of steel coils of a heating tube furnace. *J. Min. Inst.* **2021**, *249*, 393–400. [CrossRef]
28. Palaev, A.G.; Shammazov, I.A.; Dzhemilev, E.R. Research of the impact of ultrasonic and thermal effects on oil to reduce its viscosity. *J. Phys. Conf. Ser.* **2020**, *1679*, 052073. [CrossRef]
29. Zohrevand, M.; Aghaie-Khafri, M.; Forouzan, F.; Vuorinen, E. Softening mechanisms in ultrasonic treatment of deformed austenitic stainless steel. *Ultrasonics* **2021**, *116*, 106519. [CrossRef]
30. Liu, C.; Lin, C.; Liu, W.; Wang, S.; Chen, Y.; Wang, J.; Wang, J. Effects of local ultrasonic impact treatment on residual stress in an engineering-scale stainless steel pipe girth weld. *Int. J. Press. Vessel. Pip.* **2021**, *192*, 104420. [CrossRef]
31. Zhang, Y.; Jiang, X.; Fang, Y.; Fang, Y.; Liu, B.; Sun, H.; Song, T. Research and development of welding methods and welding mechanism of high-entropy alloys: A review. *Mater. Today Commun.* **2021**, *28*, 102503. [CrossRef]
32. Wang, Z.; Jiang, D.; Wu, J.; Xu, M. A review on high-frequency pulsed arc welding. *J. Manuf. Process.* **2020**, *60*, 503–519. [CrossRef]
33. Stepanova, L.N.; Kuten, M.M.; Bobrov, A.L. Using Amplitude Analysis of Acoustic Emission Signals under Cyclic and Static Loading of Steel Samples. *Russ. J. Nondestr. Test.* **2021**, *57*, 753–761. [CrossRef]
34. Stepanova, L.N.; Ramazanov, I.S.; Kireenko, V.V. The development of a defect-rejection procedure for multiple-pass welding by the distribution of the principal parameters of acoustic-emission signals. *Russ. J. Nondestr. Test.* **2014**, *50*, 667–678. [CrossRef]
35. Verzhbitskiy, K.D. Ensuring the Resource of a Vertical Steel Tank by Additional Processing of Welded Joints of the Lower Chord. Ph.D. Thesis, Saint-Petersburg Mining University, Saint Petersburg, Russia, 6 June 2019.